ELSEVIER

NeuroImage

www.elsevier.com/locate/ynimg
NeuroImage 29 (2006) 923 – 929

Human brain structures related to plantar vibrotactile stimulation: A functional magnetic resonance imaging study ☆

Stefan M. Golaszewski,[a,b,i,*] Christian M. Siedentopf,[a,b] Florian Koppelstaetter,[a,b] Martin Fend,[c] Anja Ischebeck,[d] Vicente Gonzalez-Felipe,[e] Ilka Haala,[a,b] Walter Struhal,[f] Felix M. Mottaghy,[g] Eugen Gallasch,[c] Stephan R. Felber,[a] and Franz Gerstenbrand [h]

[a]*Department of Neuroradiology, Medical University Innsbruck, Austria*
[b]*fMRI Lab, Dept. of Psychiatry, Medical University Innsbruck, Austria*
[c]*Institute of Physiology, Medical University Graz, Austria*
[d]*Department of Neurology, Medical University Innsbruck, Austria*
[e]*Institute of Medicine, Research Center Jülich, Germany*
[f]*Kaiser Franz Josef Hospital, Vienna, Austria*
[g]*Department of Nuclear Medicine, University Hospital Ulm, Germany*
[h]*Ludwig Boltzmann Institute for Restorative Neurology and Neuromodulation, Vienna, Austria*
[i]*Paracelsus Medical University Salzburg, Austria*

Received 28 April 2005; revised 3 July 2005; accepted 23 August 2005
Available online 25 October 2005

The purpose of this study was to investigate the sensorimotor cortex response to plantar vibrotactile stimulation using a newly developed MRI compatible vibration device.

Ten healthy subjects (20–45 years) were investigated. Vibrotactile stimulation of the sole of the foot with a frequency of 50 Hz and a displacement of 1 mm was performed during fMRI (echo-planar imaging sequence at 1.5 T) using an MRI compatible moving magnet actuator that is able to produce vibration frequencies between 0 and 100 Hz and displacement amplitudes between 0 and 4 mm.

The fMRI measurement during vibrotactile stimulation of the right foot revealed brain activation contralaterally within the primary sensorimotor cortex, bilaterally within the secondary somatosensory cortex, bilaterally within the superior temporal, inferior parietal, and posterior insular region, bilaterally within the anterior and posterior cingular gyrus, bilaterally within the thalamus and caudate nucleus, contralaterally within the lentiform nucleus, and bilaterally within the anterior and posterior cerebellar lobe.

The advantages of the new MRI compatible vibration device include effective transmission of the stimulus and controlled vibration amplitudes, frequencies, and intensities. The results indicate that plantar vibration can be a suitable paradigm to observe activation within the sensorimotor network in fMRI. Furthermore, the method may be used to determine the optimal responsiveness of the individual sensorimotor network.

Keywords: Functional MRI; Vibrotactile stimulation of the sole of the foot; Sensorimotor cortex for the lower extremity

Introduction

Functional magnetic resonance imaging (fMRI) is a promising tool for the mapping of the sensorimotor cortex suitable for the assessment of a large variety of neurological and neurosurgical indications. Active motor paradigms such as finger-to-thumb or foot tapping are not appropriate for the functional assessment of the sensorimotor network in case of paretic or plegic extremities. Previous PET studies have shown that continuous vibrotactile stimulation of the hand palm increases regional cerebral blood flow (rCBF) within the sensorimotor cortex (Fox et al., 1987; Seitz and Roland, 1992). Previous fMRI studies report brain activation within the primary and secondary somatosensory cortex (S1 and S2) elicited by vibrotactile stimulation (Gelnar et al., 1998; Disbrow et al., 2000) and within the motor cortex (Francis et al., 2000; Harrington et al., 2000; Golaszewski et al., 2002a,b). Therefore, vibrotactile stimulation is a suitable paradigm to probe the nature and function of the sensorimotor cortex in functional brain imaging.

Realization of mechanical vibration within the MRI environment is difficult because the use of ferromagnetic materials can be

☆ This project was supported by an Austrian National Bank grant (project number 10109).

* Corresponding author. Department of Neuroradiology, Medical University Innsbruck, Anichstrasse 35, 6020 Innsbruck, Austria. Fax: +43 512 504 23973.
E-mail address: Stefan.Golaszewski@uibk.ac.at (S.M. Golaszewski).

Available online on ScienceDirect (www.sciencedirect.com).

1053-8119/$ - see front matter © 2005 Elsevier Inc. All rights reserved.
doi:10.1016/j.neuroimage.2005.08.052

hazardous and the electric circuitry of the motors can interfere with the imaging apparatus. For sensorimotor mapping, however, well-controlled and reproducible mechanical stimuli are required. For hand and finger regions, various MRI compatible stimulation devices have been developed. For example, pneumatically driven air bags (Stippich et al., 1999; Golaszewski et al., 2002a), piezodiscs (Maldjian et al., 1999a,b; Harrington et al., 2000), cable-driven rotating masses (Golaszewski et al., 2002b), and coil designs that utilize the scanner internal static magnetic field (Graham et al., 2001). For plantar stimulation, however, these devices are less suited.

Under normal conditions, the sole tissue experiences either pressure that is steady (standing) or variable (walking), while transient vibrotactile stimuli occur. Thus, for the stimulation of sole receptors, a device is needed that simultaneously delivers a predefined static force and vibration. The surface compliance at the sole is also much smaller than that at the palm of the hand. Therefore, more intense vibrotactile stimuli are needed for the foot to elicit sensorimotor responses.

The long distance between sole receptors (outside the scanner) and the brain (inside the scanner) allows the use of electromagnetic devices. Noncommutated devices such as moving coils and moving magnets that produce no HF emissions during operation are suited. These actuator types are linear in their control characteristic, which is ideal for a multipurpose stimulator. In this paper, we describe a stationary moving magnet actuator connected to an indentor to contact and vibrate the sole of the foot. Special attention was put on the control of the actuator to allow independent settings of contact force and vibration. There was no interference between the moving magnet actuator and the MRI system.

The first aim of the study was to design and construct a MRI compatible vibrotactile stimulation device for the stimulation of the sole of the foot. The second aim was to map in detail the cerebral structures that exhibited changes of the BOLD (blood oxygenation level dependent) response during stimulation.

Materials and methods

Ten healthy, right-handed male volunteers with dominance of the right hand (age range between 20 and 45 years, mean age 27 years) without any history of neurological or psychiatric disorders or drug abuse participated in this study. None of them was on any medication. All subjects gave written consent. The ethical committee of the Medical School of Innsbruck, Austria, approved the study protocol.

Moving magnet actuator system (MMAS) with controller

A commercially available moving magnet actuator system with a maximum stroke of 19 mm and a maximum force of 20 N (Type LMNM2-1F5-F8, Baldor Inc., USA) was selected as vibration device. This actuator type is highly back drivable, which means that practically no friction is produced when the magnet is moved by external forces. This feature allows the generation of position-independent forces which is advantageous to keep the indentor in contact with the foot sole during vibration and at small foot displacements.

For independent setting of contact force and vibration, a velocity feedback controller was implemented. This controller consists of a velocity feedback loop including a second input in the forward control path for setting the contact force. As the contact force is of static nature (0–1 Hz), the second input signal does not conflict with the vibration control (20–100 Hz). This controller was implemented by a software running on a standard PC (SUSE LINUX operating system with RT-kernel, 5-kHz process cycle). The control signals were digitized by 16 bit AD/DA converters and interfaced to the PC parallel port.

To test the performance of the implemented controller, pieces of foam rubber with similar mechanical properties as sole tissue were indented and vibrated. The vibration frequency was varied between 20 and 100 Hz, the given amplitude was 0.4 or 1 mm, respectively. To study the influence of the contact force on the vibration amplitude, three static force levels, 2, 5, and 10 N were tested. Without velocity feedback (open loop), the vibration amplitude highly depended on frequency and contact force. With velocity feedback (closed loop), the force dependence became minimal, and an almost linear frequency response between 20 and 100 Hz was achieved.

The complete stimulation hardware consisted of the platform with foot supports, stimulators, cables, IN/OUT-unit, and PC. In order to avoid mechanical resonance, the platform was made from a 10-mm aluminum plate. The lower side of the platform was equipped with rubber elements, which fit into the sled of the MRI scanner. Two supports, one for the ankle and one for the foot, were used to keep the leg in a relaxed and stable position. Both supports were equipped with Welcro bands for quick and comfortable leg fixation. Exchangeable foot-shaped plexiglas plates with 30 mm holes were used to contact the sole by the indentor (see Fig. 1).

The stimulation software includes features for stimulus synthesis and sequencing, as well as master–slave and communication capabilities. In the case of simple block designs, the stimulator can be operated without continuous synchronization with the MRI scanning sequence. However, for event-related designs (Dale and Buckner, 1997), continuous synchronization between stimulus presentation and the scanning sequence on the basis of the scanner trigger signal is required. For stimulus presentation and synchro-

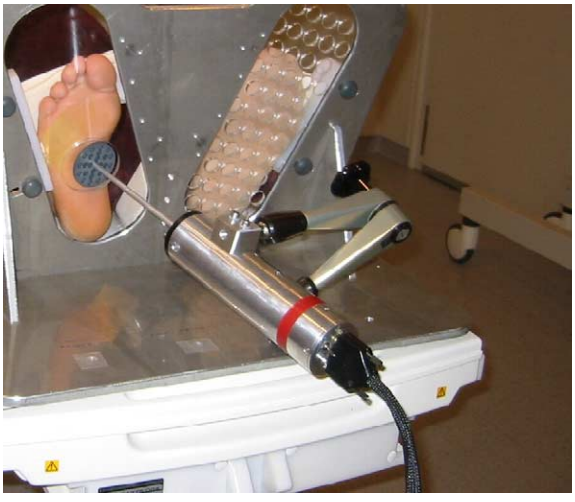

Fig. 1. Vibration probe attached to the subject's arch of the foot with a contact force of 0.05 N to the skin surface. The contact area of the skin surface and the indentor was circular and about 20 cm^2. The Moving Magnet Actuator System was regulated, so that the contact force was kept constant at 0.05 N throughout the fMRI measurement.

nization, the Software Presentation® (Presentation Software, Neurobehavioralsystems Inc., California) was used. To allow synchronization, the stimulator is operated in the slave mode. For master–slave operation, a software communication protocol with codes for stimulus frequency, amplitude, and contact force was defined.

Experimental procedure

The subjects were instructed to lie relaxed with their hands resting upon the abdomen and to keep their eyes closed during the fMRI measurement. Foam padding and a special helmet fixed to the head coil was used in order to limit involuntary head motions. The vibration probe was positioned and attached to the arch of the subject's right foot with a contact force of 0.05 N to the skin surface (Fig. 1). The contact area between the skin surface and the indentor was circular and exactly 19.63 cm^2 (diameter 5 cm), as measured by the method of Brisben et al. (1999). The moving magnet actuator system (MMAS) was regulated so that the contact force was kept constant at 0.05 N throughout the fMRI measurement.

A test vibration procedure was carried out inside the MRI scanner to ensure that the vibration device did not influence the quality of the echo-planar images. The cables of the vibration device were completely shielded, and the moving magnet actuator was placed exactly at the 20-mT isoline of the static magnetic field of the MRI scanner. With this experimental setup, no interference between the vibration device and the MRI measurement and vice versa was detectable. Vibrotactile stimuli with a frequency of 50 Hz and amplitude of 1 mm were presented in an event-related fMRI design.

MRI

Experiments were performed on a 1.5-T whole body scanner (Magnetom SONATA, Siemens, Germany) with an echo-planar capable gradient system (rise time 300 μs, gradient strength 25 mT/ms) and a circular polarized head coil (FoV = 250 mm). For fMRI, we employed T2*-weighted single shot echo-planar sequences (TR/TE/α = 0.96 ms/66 ms/90°, matrix = 64 × 64, inplane resolution 3.75 × 3.75 mm, thickness: 5 mm, gap: 1.25 mm) (Ogawa et al., 1990; Kwong et al., 1992; Ogawa et al., 1992; Kwong, 1995). 24 axial slices parallel to the bicommissural plane were acquired. The scan repetition time (TR) was 2.5 s including a delay of 50 ms. The duration of the entire fMRI measurement was 736 scans inclusive of 5 dummy scans resulting in a total scan time of 30.67 min.

A pilot study employing a block design showed less extent of the cortical activation and smaller t values than the event-related designed study. Therefore, to avoid adaptation phenomena and to increase the robustness of the cortical and subcortical BOLD response, we implemented the vibration paradigm in event-related design technique, where a series of single event stimuli within a variable interstimulus interval was applied (Dale and Buckner, 1997). A stimulation condition (50 Hz, 1 mm amplitude) and one baseline condition (no stimulation) were used. The sequence of stimuli was randomized for each subject. Stimulus duration was 1 s. On average, every 7 s, a stimulus was presented. Per subject, 736 volume images were acquired during the run. The first five images of each time series were discarded from the analysis to allow magnetization to reach equilibrium.

Image analysis

Image analysis was performed with SPM99 (The Welcome Department of Cognitive Neurology, http://www.fil.ion.ucl.ac.uk/spm). The time series of images was realigned to the first image of the time series to correct for head motion. High pass filtering (cutoff period 50 s) was performed to eliminate low-frequency scanner drifts. The functional images were normalized using the MNI (Montreal Neurological Institute) template. Afterwards, the volume images were spatially smoothed using an isotropic Gaussian kernel (8 mm FWHM). The model time course of the signal was generated by convolving the stimulus onsets of each condition with the canonical form of the HRF and its first derivative as given in SPM99. Linear t contrasts were specified for between condition comparisons. The contrast images from the individual subjects analysis were used to calculate a fixed effects group analysis. Clusters are reported as being significant if they passed an uncorrected threshold of $P < 0.001$ with a corrected P value on cluster level of less than 0.05. Anatomical location of the activation foci was determined using the atlas of Talairach and Tournoux (1988). The secondary somatosensory cortex (S2) was defined according to the atlas of Affifi and Bergman (1998) and Nirkko et al. (2001) as an area located on the most inferior aspect of the postcentral gyrus and in the superior bank of the lateral sulcus within the parietal operculum.

Results

The contrast vibrotactile stimulation versus baseline (no stimulation) revealed activation within the secondary somatosensory cortex S2, the inferior parietal lobule (BA 39 contralaterally, 40 and 43 bilaterally), the superior parietal lobule (precuneus, BA 5 and 7 bilaterally with a dominance of the left side), the anterior and posterior cingular gyrus (BA 23, 24, 29, and 31 bilaterally), and the left posterior insula (BA 13). Additional activation was observed bilaterally within the thalamus and caudate nucleus as well as the anterior (culmen) and posterior (declive) cerebellar lobe. Activation within the thalamus included the pulvinar, the lateral dorsal nucleus, the lateral posterior nucleus, the midline nucleus, the ventral posterior lateral nucleus, the ventral posterior medial nucleus, and the ventral lateral nucleus. Contralaterally to the stimulated foot, responses within the primary sensorimotor cortex including the pre- and postcentral gyrus (SM1; BA 1, 2, 3a, 3b, 4) and the lentiform nucleus were seen (see Table 1, Fig. 2).

Discussion

In the present study, the feasibility of a newly designed vibrotactile plantar stimulator and corresponding BOLD responses in fMRI were shown.

Microneurographic recordings from the glabrous skin of the foot sole identified four different types of cutaneous mechanoreceptors within the cutis and subcutis with low thresholds, the slowly adapting (SA) receptors type I and type II (Merkel and Ruffinian receptors) and the rapidly adapting (RA) receptors type I and II (Meissner and Pacinian receptors) (Johansson, 1976, 1978; Vallbo et al., 1979; Knibestöl, 1973, 1975; Kennedy and Inglis, 2002). The lowest physical and psychophysical thresholds of the cutaneous mechanoreceptors can be found within the medial ball

Table 1
Activation clusters detected for the contrasts of the images acquired during vibrotactile stimulation and the resting condition

Anatomical location		BA	*P* value	*t* value	Cluster size	MNI coordinates of max. *t* value		
						x	*y*	*z*
L	**Postcentral gyrus**	**1, 2, 3a, 3b**	**0.0001**	**8.84**	265	**− 12**	**− 44**	**72**
L	Precentral gyrus	4						
L	Precuneus	7						
L	Sup. parietal lobule	5						
R	Precuneus	7						
R	Sup. parietal lobule	5						
L	Post. cingular gyrus	23, 24, 31						
R	Post. cingular gyrus	23, 24, 31						
L	**Post. Insula**	**13**	**0.0001**	**7.01**	**729**	**− 32**	**− 24**	**8**
L	Postcentral gyrus	43						
L	Inf. parietal lobule	39, 40						
L	Cingular gyrus	29						
R	Cingular gyrus	29						
L	Thalamus							
L	Caudate nucleus							
R	Thalamus							
R	Caudate nucleus							
L	Lentiform nucleus							
R	**Ant. cingular gyrus**	**24**	**0.009**	**4.90**	**26**	**0**	**28**	**12**
R	**Postcentral gyrus**	**40**	**0.001**	**4.71**	**39**	**56**	**− 28**	**20**
R	Postcentral gyrus	43						
L	**Left cerebellar hemisphere**		**0.0001**	**6.67**	**58**	**− 36**	**− 68**	**− 24**
R	**Right cerebellar hemisphere**		**0.013**	**5.29**	**24**	**36**	**− 64**	**− 24**

BOLD responses are reported for clusters that surpassed an uncorrected threshold of $P < 0.001$ and a corrected P value of $P < 0.05$ on cluster level, corrected for multiple comparisons. BA = Brodmann Area; R = right hemisphere; L = left hemisphere; MNI = Montreal Neurological Institute.

and the medial arch of the foot (Inglis et al., 2002) that has only a thin layer of horny skin. Therefore, the vibration probe was attached to the glabrous skin onto the medial arch of the foot with a preload of 0.05 N (Kennedy and Inglis, 2002). The different receptor types are randomly distributed throughout the plantar surface of the foot and are primarily involved in weight-bearing actions, standing balance, and movement control. The used vibration frequency of 50 Hz is in the upper range of the

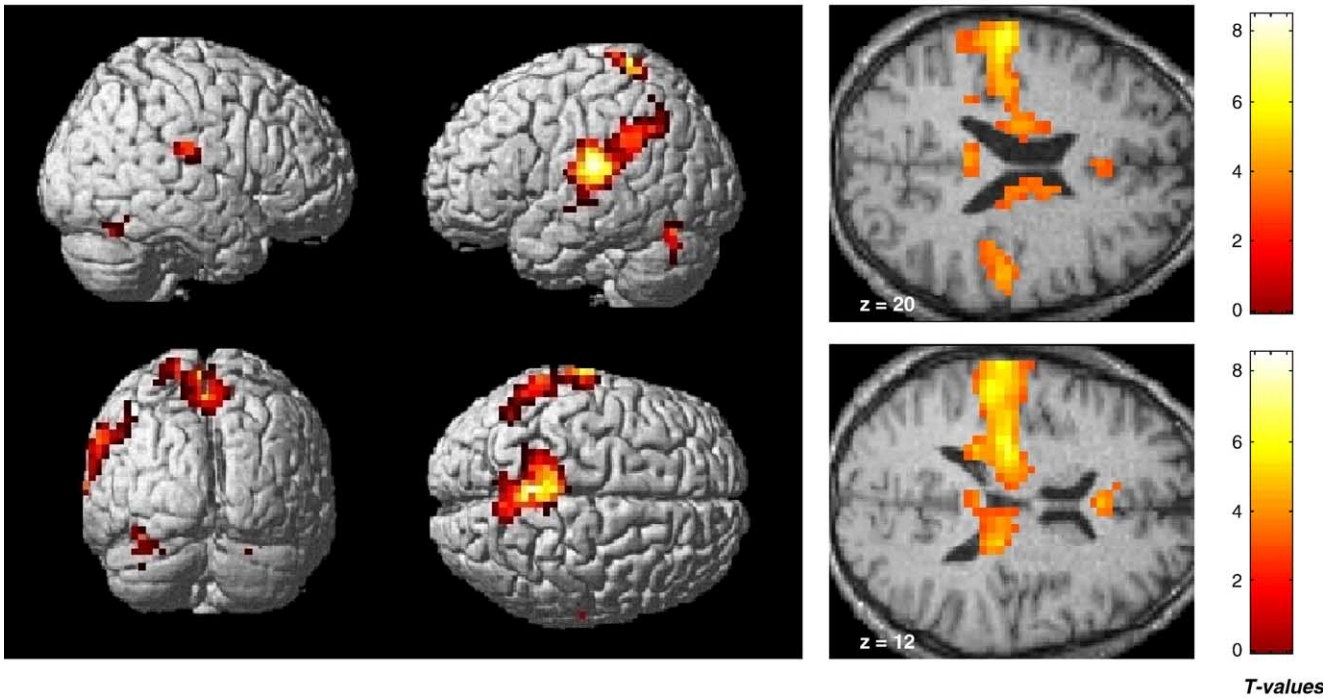

Fig. 2. Surface rendering and volume rendering of the fMRI map for vibrotactile stimulation of the foot sole (50 Hz, 1 mm amplitude, sinusoidal stimulus): fMRI group data of 10 subjects. Clusters are reported as being significant if they passed an uncorrected threshold of $P < 0.001$ with a corrected P value on cluster level of less than 0.05, corrected for multiple comparisons.

Meissner's corpuscle scale and in the lower range of the Pacinian corpuscle scale to address both vibration-sensitive receptor types (Harrington et al., 2001). A vibration amplitude of 1 mm was applied to reach mechanical deformations of the tissue beyond the dermis and subcutis also in the bellies of the small muscles of the foot to activate primary and secondary muscle spindle endings as well as Golgi tendon organs. Thus, besides the exteroceptive input from the cutaneous mechanoreceptors, additional proprioceptive input to the brain was elicited (Moore et al., 2000; Iwamura et al., 1993; Ibañez et al., 1989; Kaas et al., 1979; Maldjian et al., 1999a,b; Recanzone et al., 1992).

In the present study, bilateral BOLD response with a lateralization to the left side could be detected within the thalamus including the ventral posterior lateral nucleus (VPL), the ventral posterior medial nucleus (VPM), the pulvinar (P), the lateral dorsal nucleus (LD), the lateral posterior nucleus (LP), the midline nucleus (M), and the ventral lateral nucleus (VL). Epicritic somatosensory information from extero- and proprioception targets especially the contralateral VPL.

From the thalamus, there is a wide projection to the neocortex as reported in previous studies (Merzenich et al., 1981; Fisher et al., 1983; Fox et al., 1987; Burton and Sinclair, 1991; Seitz and Roland, 1992; Francis et al., 2000; Golaszewski et al., 2002a,b). An extensive activation focus could be located contralaterally to the stimulated foot within the primary somatosensory cortex (S1). Contralateral S1 response is expected since each subregion of S1 (BA 3a, b, 2, 1) receives input from primarily one type of receptor (Geyer et al., 1999; Kurth et al., 2000). In BA 3a, the dominant input originates from proprioceptors signaling muscle stretch. BA 3b receives input primarily from the cutaneous mechanoreceptors. In BA 1, the input of rapidly adapting cutaneous mechanoreceptors predominates. BA 2 receives convergent input from slowly and rapidly adapting cutaneous mechanoreceptors and proprioceptors. Mountcastle et al. demonstrated that Meissner's corpuscles project primarily contralaterally into BA 3b and 1 (Mountcastle et al., 1969), and Ferrington et al. described that Pacinian corpuscles project diffusely contralaterally into BA 3a and 2 and bilaterally into S2, especially into BA 40 (Ferrington and Rowe, 1980; Gelnar et al., 1998; Maldjian et al., 1999a,b; Francis et al., 2000). This network of brain regions could also be demonstrated to be targeted by vibrotactile stimulation in the current study.

S2 involvement by plantar vibrotactile stimulation is explained by the known mainly feed forward connections between S1 and S2 and mainly originates from projections from BA 1 and 2. S2 was activated bilaterally with a lateralization to the left side. A bilateral response in S2 to vibrotactile stimulation of the hand was also described in studies with somatosensory-evoked potentials (Hamalainen et al., 1990; Kany and Treede, 1997) as well as in PET studies (Burton et al., 1993; Seitz and Roland, 1992). For the ipsilateral S2 response, thalamocortical or transcallosal projections are discussed (Burton et al., 1993; Seitz and Roland, 1992). S2 projects to the insular cortex, which in turn innervates regions of the temporal lobe believed to be important for tactile memory. Accordingly, the posterior insular region (BA 13) responded to vibrotactile stimulation.

The third major subdivision of the somatosensory cortex, the posterior parietal cortex (BA 5 and 7), was activated bilaterally, too. The posterior parietal cortices of both hemispheres receive input from S1 as well as input from the pulvinar and thus have an associative function. Both are also connected through the corpus callosum. BA 5 integrates tactile information from mechanoreceptors in the skin with proprioceptive input from the underlying muscles and joints. BA 7 receives visual as well as tactile and proprioceptive input, allowing integration of stereognostic and visual information. The posterior parietal cortex projects to the motor areas of the frontal lobe and plays an important role in sensory initiation and guidance of movement.

Also neuronal activation within motor centers, especially contralaterally within the primary motor cortex (M1, BA 4), could be detected. The motor response to vibration is most probably evoked by transcortical loops (Evarts, 1973; Murphy et al., 1975), which are involved in the vibratory tonic reflex (VTR) or direct thalamocortical projections (Golaszewski et al., 2002b). The BOLD response within the primary motor cortex M1 could be elicited by direct extero- and proprioceptive projections. Direct afferent projections to M1 have been described (Goldring and Ratcheson, 1972; Lucier et al., 1975; Hore et al., 1976; Asanuma et al., 1980; Murphy et al., 1975). The applied vibrotactile stimulus induces repetitive short stretches within the small muscles of the foot eliciting cortical long loop reflexes and thus involves M1. Furthermore, the vibratory tonic reflex in the bellies of the flexors of the digits I–V as well as in the bellies of the small muscles of the sole of the right foot is elicited (Burke et al., 1976; Golaszewski et al., 2002b).

The right parietal inferior and anterior cingular response are most likely associated with attention attracted by the incoming somatosensory information. Response within network components of the Papez circuit – an important circuitry for emotional processing of afferent somatosensory signals – as the medial thalamic and the posterior cingular region maybe the fMRI correlate of an involvement of the emotional assessment of the vibrotactile stimuli. The bilateral cerebellar response within the anterior and posterior lobe can be taken as projections of the spinocerebellar tract. Response bilaterally within the caudate nucleus and contralaterally within the lentiform nucleus, especially the putamen, indicates an involvement of basal ganglia into the subcortical processing of afferent somatosensory stimuli.

The presented stationary moving magnet actuator is a non-commutated device which produces no HF emissions during operation. It therefore does not interfere with the imaging apparatus. To elucidate potential differences in somatosensory brain activation produced by different classes of superficial and deep skin receptors or proprioceptors, a main feature of the system is the independent control of indentation force, vibration amplitude, and vibration frequency. Previous vibration devices (Stippich et al., 1999; Golaszewski et al., 2002a; Maldjian et al., 1999a,b; Harrington et al., 2000; Golaszewski et al., 2002b; Graham et al., 2001) need an active motor component to contact the vibrating source which is a source for systematic errors. Such errors are further reduced by feedback control. The skin surface of the human foot cannot be completely immobilized. There are continuous fluctuations related to cardiac and respiratory events. The amplitudes of these movements and the thresholds of the cutaneous mechanoreceptors may introduce considerable variability in effective stimulus amplitude and indentation force. To overcome this difficulty, the vibration stimulator was constructed with the facility to present the desired amplitude and indentation force of the vibration stimulus while controlling for the movements of the skin surface relative to the stimulator (Westling et al., 1976). The vibration amplitude was conserved against responding tissue forces and was constant throughout the measurement. The vibrotactile

stimuli were applied with a constant preload of 0.05 N. Therefore, the presented system has the capability to deliver precisely controlled, exactly reproducible vibrotactile stimuli with frequencies between 0 and 100 Hz and displacement amplitudes between 0 and 4 mm. Thus, variability in time series data can be reduced improving fMRI brain mapping. This can further be improved by using correlation or fitting methods that make a priori assumptions about the idealized hemodynamic response produced by neuronal activation during fMRI experiments. At least, it is also possible to quantify plantar stiffness by measurement of the indentation depth at a given force. This is an important feature for the establishment of quantitative stimulus–response relationships as a reference for diagnostic procedures.

The applied vibrotactile stimulus elicits neuronal activation within a wide network of cortical and subcortical structures, a fact that holds promise for the applicability in functional diagnosis of the brain such as preoperative functional mapping of the sensorimotor cortex in patients with brain tumors. Further applications include the investigation of brain plasticity and reorganization in neurorehabilitation (Pons et al., 1992) and the investigation of patients in comatose or vegetative state (Kampfl et al., 1998; Laureys et al., 2002). Besides, the vibration paradigm holds promise for probing the afferent pathways especially in gait disorders (e.g., diabetes mellitus) or spinal cord injury. Further studies are necessary to investigate the dependence of the BOLD response from the vibration frequency (Tommerdahl et al., 1999; Maldjian et al., 1999a,b; Francis et al., 2000) and the vibration amplitude (Nelson et al., 2004).

Acknowledgments

The authors wish to express their gratitude to Prof. Dr. Milan Dimitrijevic from the Baylor College of Houston, Texas, for his continuous support and advice for the preparation of the study and Dr. techn. Michael Hackel for the implementation of the computer network for fMRI data analysis.

References

Affifi, A.K., Bergman, R.A., 1998. Functional Neuroanatomy, Text and Atlas. McGraw-Hill.

Asanuma, H., Larsen, K., Yumiya, H., 1980. Peripheral input pathways to the monkey motor cortex. Exp. Brain Res. 38, 349–355.

Brisben, A.J., Hsiao, S.S., Johnson, K.O., 1999. Detection of vibration transmitted through an object grasped in the hand. J. Neurophysiol. 81 (4), 1548–1558.

Burke, D., Hagbarth, K.E., Löfstedt, L., et al., 1976. The response of human muscle spindle endings to vibration of non-contracting muscles. J. Physiol. 261, 673–693.

Burton, H., Sinclair, R.J., 1991. Second somatosensory cortical area in macaque monkeys: 2. Neuronal response to punctuate vibrotactile stimulation of glabrous skin on the hand. Brain Res. 538, 127–135.

Burton, H., Videen, T.O., Raichle, M.E., 1993. Tactile-vibration-activated foci in insular and parietal–opercular cortex studied with positron emission tomography: mapping the second somatosensory area in humans. Somatosens. Motor Res. 10 (3), 297–308.

Dale, A., Buckner, R., 1997. Selective averaging of rapidly presented individual trails using fMRI. Hum. Brain Mapp. 5, 329–340.

Disbrow, E., Roberts, T., Krubitzer, L., 2000. Somatotopic organization of cortical fields in the lateral sulcus of Homo sapiens: evidence for SII and PV. J. Comp. Neurol. 418 (1), 1–21.

Evarts, E.V., 1973. Motor cortex reflexes associated with learned movement. Science 179 (72), 501–503.

Ferrington, D.G., Rowe, M., 1980. Differential contributions to coding of cutaneous vibratory information by cortical somatosensory areas I and II. J. Neurophysiol. 43, 310–331.

Fisher, G.R., Freeman, B., Row, M.J., 1983. Organization of parallel projections from Pacinian afferent fibers to somatosensory cortical areas I and II in cat. J. Neurophysiol. 43, 75–97.

Fox, P.T., Burton, H., Raichle, M.E., 1987. Mapping human somatosensory cortex with positron emission tomography. J. Neurosurg. 67, 34–43.

Francis, S.T., Kelly, E.F., Bowtell, R., Dunseath, W.J., Folger, S.E., McGlone, F., 2000. fMRI of the responses to vibratory stimulation of digit tips. NeuroImage 11 (3), 188–202.

Gelnar, P.A., Krauss, B.R., Szeverenyi, N.M., et al., 1998. Fingertip representation in the human somatosensory cortex: an fMRI study. NeuroImage 7, 261–283.

Geyer, S., Schleicher, A., Zilles, K., 1999. Areas 3a, 3b, and 1 of human primary somatosensory cortex: Part 1. Micro structural organization and interindividual variabilities. NeuroImage 10 (1), 63–83.

Golaszewski, S.M., Zschiegner, F., Siedentopf, C.M., Unterrainer, J., Sweeney, R.A., Eisner, W., Unterrainer, J., Lechner-Steinleitner, S., Mottaghy, F.M., Felber, S., 2002a. A new pneumatic vibrator for functional magnetic resonance imaging of the human sensorimotor cortex. Neurosci. Lett. 324, 125–128.

Golaszewski, S.M., Siedentopf, C.M., Baldauf, E., Koppelstaetter, F., Eisner, W., Unterrainer, J., Guendisch, G.M., Mottaghy, F.M., Felber, S.R., 2002b. Functional magnetic resonance imaging of the human sensorimotor cortex using a novel vibrotactile stimulator. NeuroImage 17, 421–430.

Goldring, S., Ratcheson, R., 1972. Human motor cortex: sensory input data from single neuron recordings. Science 175, 1493–1495.

Graham, S.J., Staines, W.R., Nelson, A., Plewes, D.B., McIlroy, W.E., 2001. New devices to deliver somatosensory stimuli during functional MRI. Magn. Reson. Med. 46 (3), 436–442.

Hamalainen, H., Kekoni, J., Sams, M., Reinukainen, K., Naatanen, T., 1990. Human somatosensory evoked potentials to mechanical pulses and vibrations: contributions of SI and SII somatosensory cortices to P50 and P100 components. Electroencephalogr. Clin. Neurophysiol. 75, 12–21.

Harrington, G.S., Wright, C.T., Downs III, J.H., et al., 2000. A new vibrotactile stimulator for functional MRI. Hum. Brain Mapp. 3, 140–145.

Harrington, G.S., Hunter III, D.J., et al., 2001. FMRI mapping of the somatosensory cortex with vibratory stimuli. Is there a dependency on stimulus frequency? Brain Res. 897 (1–2), 188–192.

Hore, J., Preston, J.B., Cheney, P.D., 1976. Responses of cortical neurons (areas 3a and 4) to ramp stretch of hind limb muscles in the baboon. J. Neurophysiol. 39, 484–500.

Ibañez, V., Deiber, M.P., Mauguière, F., et al., 1989. Interference of vibrations with input transmission in dorsal horn and cuneate nucleus in man: a study of somatosensory evoked potentials (SEPs) to electrical stimulation of median nerve and fingers. Exp. Brain Res. 75, 599–610.

Inglis, J.T., Kennedy, P.M., Wells, C., Chua, R., 2002. The role of cutaneous receptors in the foot. Adv. Exp. Med. Biol. 508, 111–117.

Iwamura, Y., Tanaka, M., Sakamoto, M., Hikosaka, O., 1993. Rostrocaudal gradients in the neuronal receptive field complexity in the finger region of the alert monkey's postcentral gyrus. Exp. Brain Res. 92 (3), 360–368.

Johansson, R.S., 1976. Skin mechanoreceptors in the human hand: receptive field characteristics. In: Zotterman, Y. (Ed.), Sensory Functions of the Skin in Primates. Pergamon, Oxford, pp. 159–170.

Johansson, R.S., 1978. Tactile sensibility in the human hand: receptive field characteristics of mechanoreceptor units in the glabrous skin. J. Physiol. (London) 281, 101–123.

Kaas, J.H., Nelson, R.J., Sur, M., Lin, C.S., Merzenich, M.M., 1979. Multiple representations of the body within the primary somatosensory cortex of primates. Science 204 (4392), 521–523.

Kampfl, A., Schmutzhard, E., Franz, G., et al., 1998. Prediction of recovery from post-traumatic vegetative state with cerebral magnetic resonance imaging. Lancet 35, 1763–1767.

Kany, C., Treede, R., 1997. Median and tibial nerve somatosensory evoked potentials: middle-latency components from the vicinity of the secondary somatosensory cortex in humans. Electroencephalogr. Clin. Neurophysiol. 10, 402–410.

Kennedy, P.M., Inglis, J.T., 2002. Distribution and behaviour of glabrous cutaneous receptors in the human foot sole. J. Physiol. 538 (Pt 3), 995–1002.

Knibestöl, M., 1973. Stimulus–response functions of rapidly adapting mechanoreceptors in human glabrous skin area. J. Physiol. 232 (3), 427–452.

Knibestöl, M., 1975. Stimulus–response functions of slowly adapting mechanoreceptors in the human glabrous skin area. J. Physiol. 245 (1), 63–80.

Kurth, R., Villringer, K., Curio, G., Wolf, K.J., Krause, T., Repenthin, J., Schwiemann, J., Deuchert, M., Villringer, A., 2000. fMRI shows multiple somatotopic digit representations in human primary somatosensory cortex. NeuroReport 11 (7), 1487–1491.

Kwong, K.K., 1995. Functional magnetic resonance imaging with echo planar imaging. Magn. Reson. Q. 11, 1–20.

Kwong, K.K., Belliveau, J.W., Chesler, D.A., et al., 1992. Dynamic magnetic resonance imaging of human brain activity during primary sensory stimulation. Proc. Natl. Acad. Sci. U. S. A. 89, 5675–5679.

Laureys, S., Faymonville, M.E., Peigneux, P., Damas, P., Lambermont, B., Del Fiore, G., Degueldre, C., Aerts, J., Luxen, A., Franck, G., Lamy, M., Moonen, G., Maquet, P., 2002. Cortical processing of noxious somatosensory stimuli in the persistent vegetative state. NeuroImage 17 (2), 732–741.

Lucier, G.E., Rüegg, D.C., Wiesendanger, M., 1975. Responses of neurons in motor cortex and in area 3A to controlled stretches of forelimb muscles in cebus monkey. J. Physiol. (London) 251, 833–853.

Maldjian, J.A., Gottschalk, A., Patel, R.S., Detre, J.A., Alsop, D.C., 1999a. The sensory somatotopic map of the human hand demonstrated at 4 Tesla. NeuroImage 10 (1), 55–62.

Maldjian, J.A., Gottschalk, A., Patel, R.S., Pincus, D., Detre, J.A., Alsop, D.C., 1999b. Mapping of secondary somatosensory cortex activation induced by vibrational stimulation: an fMRI study. Brain Res. 824, 291–295.

Merzenich, M.M., Sur, M., Nelson, R.J., Kaas, J.H., 1981. Organization of the SI cortex: multiple cutaneous representations in area 3b and 1 of the owl monkey. In: Woolsey, C.N. (Ed.), Cortical Sensory Organization, vol. 1. Humana Press, pp. 36–48.

Moore, C.I., Stern, C.E., Corkin, S., Fischl, B., Gray, A.C., Rosen, B.C., Dale, A.M., 2000. Segregation of somatosensory activation in the human rolandic cortex using fMRI. J. Neurophysiol. 84 (1), 558–569.

Mountcastle, V.B., Talbot, W.H., Sakata, H., et al., 1969. Cortical neuronal mechanisms in flutter-vibration studied anaesthetized monkeys: neural periodicity and frequency discrimination. J. Neurophysiol. 32, 452–484.

Murphy, J.T., Wong, Y.C., Kwan, H.C., 1975. Afferent–efferent linkages in motor cortex for single forelimb muscles. J. Neurophysiol. 38, 990–1014.

Nelson, A.J., Staines, W.R., Graham, S.J., McIlroy, W.E., 2004. Activation in SI and SII; the influence of vibrotactile amplitude during passive and task-relevant stimulation. Cogn. Brain Res. 19, 174–184.

Nirkko, A.C., Ozdoba, C., Redmond, S.M., Burki, M., Schroth, G., Hess, C.W., Wiesendanger, M. 2001.Different ipsilateral representations for distal and proximal movements in the sensorimotor cortex: activation and deactivation patterns. NeuroImage 13 (5), 825–835.

Ogawa, S., Lee, T.M., Kay, A.R., et al., 1990. Brain magnetic resonance imaging with contrast dependant on blood oxygenation. Proc. Natl. Acad. Sci. U. S. A. 87, 9868–9872.

Ogawa, S., Tank, D.W., Menon, R., et al., 1992. Intrinsic signal changes accompanying sensory stimulation: functional brain mapping with magnetic resonance imaging. Proc. Natl. Acad. Sci. U. S. A. 89, 5951–5955.

Pons, T.P., Garraghty, P.E., Mishkin, M., 1992. Serial and parallel processing of tactual information in somatosensory cortex of rhesus monkeys. J. Neurophysiol. 68, 518–527.

Recanzone, G.H., Merzenich, M.M., Jenkins, W.M., 1992. Frequency discrimination training engaging a restricted skin surface results in an emergence of a cutaneous response zone in cortical area 3a. J. Neurophysiol. 67 (5), 1057–1070.

Seitz, R.J., Roland, P.E., 1992. Vibratory stimulation increases and decreases the regional cerebral blood flow and oxidative metabolism: a positron emission tomography (PET) study. Acta Neurol. Scand. 86, 60–67.

Stippich, C., Hofmann, R., Kapfer, D., Hempel, E., Heiland, S., Jansen, O., Sator, K., 1999. Somatotopic mapping of the human primary somatosensory cortex by fully automated tactile stimulation using functional magnetic resonance imaging. Neurosci. Lett. 277 (1), 25–28.

Talairach, J., Tournoux, P., 1988. Co-Planar Stereotaxic Atlas of the Human Brain: 3-Dimensional Proportional System: An Approach to Cerebral Imaging. Georg Thieme Verlag, Stuttgart and New York.

Tommerdahl, M., Whitsel, B.L., Favorov, O.V., Metz, C.B., O'Quinn, B.L., 1999. Responses of contralateral SI and SII in cat to same-site cutaneous flutter versus vibration. J. Neurophysiol. 82 (4), 1982–1992.

Vallbo, A.B., Hagbarth, K.E., Torebjork, H.E., Wallin, B.G., 1979. Somatosensory, proprioceptive, and sympathetic activity in human peripheral nerves. Physiol. Rev. Oct. 59 (4), 919–957.

Westling, G., Johansson, R.S., Vallbo, A.B., 1976. A method for mechanical stimulation of skin receptors. In: Zotterman, Y. (Ed.), Sensory Functions of the Skin in Primates. Pergamon, Oxford, pp. 151–158.